

Edge Electron Temperature Fluctuations and Conductive Turbulent Heat Flux in DIII-D



D.L. Rudakov,

J. A. Boedo,

R. A. Moyer

**University of California,
San Diego**

J. G. Watkins

Sandia

National Laboratories



Abstract

Fast (100 kHz bandwidth) measurements of the edge electron temperature have been performed in DIII-D using a recently installed diagnostic based on detection of harmonics generated in the current spectrum of a single Langmuir probe driven by high-frequency sinusoidal voltage. Electron temperature fluctuations with relative root-mean-square (rms) levels ranging from 0.3 - 0.5 at the separatrix to 0.5 - 0.8 in the scrape-off layer are found in both L and H modes in DIII-D. The fluctuations give rise to a turbulent conductive heat flux. Though the fluctuations are broadband with significant energy throughout the measurable range (up to 100 kHz), most of the heat transport occurs at frequencies below 50 kHz. Measured net conductive turbulent heat flux in L-mode is typically about 1 W/cm² at the separatrix, falling exponentially with the radius. Multiplied by the area of the last closed flux surface this gives about 0.8 MW of total power conducted through the separatrix, which is comparable to the difference between the total input power and the total radiated power. Conductive heat flux in H-mode is considerably lower and its contribution to the power balance is small.

Motivation for Fast Edge T_e Measurements in DIII-D

Fast measurements of the edge electron temperature are needed to:

- Measure the turbulent heat flux in the boundary of DIII-D in L and H mode
- Answer the questions:
 - * is the H-mode transport barrier primarily a particle convection barrier, or heat conduction barrier?
 - * is edge heat transport dominated by electrostatic turbulence as particle transport is?
- Evaluate errors in turbulent particle flux measurements due to neglecting T_e fluctuations
- Obtain time-resolved RMS amplitudes, cross-phases, particle and heat fluxes, to compare with predictions of analytic theory and numerical simulations

T_e Fluctuations and Turbulent Fluxes

Electron temperature fluctuations drive
turbulent conductive heat flux:

$$Q_r^{ES} = Q_{conv} + Q_{cond} = \frac{5}{2} k T_e \Gamma_r + \frac{3}{2} \frac{n_e}{B_j} \langle k \tilde{T}_e \tilde{E}_q \rangle$$

\tilde{T}_e measurements necessary to measure Q_{cond}

Neglecting T_e fluctuations may affect turbulent particle
flux measurements:

$$\Gamma_r^{ES} = \frac{1}{B_j} \langle \tilde{n} \tilde{E}_q \rangle$$

$$\tilde{E}_q = -\nabla_q \tilde{J}_p \text{ usually estimated as } \tilde{E}_q \approx -\nabla_q \tilde{J}_f$$

However, $\tilde{J}_p = \tilde{J}_f + \mathbf{a} k \tilde{T}_e / e$ where $\mathbf{a} \sim 3 \Rightarrow$ **possible large errors!**

\tilde{T}_e measurements needed for correction

Harmonic Diagnostic Basics

Current to a DC-floating probe driven by sinusoidal voltage $U = U_0 \cos(\omega t)$ can be expressed as a series of sinusoidal harmonics [1]:

$$I_{pr} = \frac{2I_{si}}{I_0\left(\frac{eU_0}{kT_e}\right)} \sum_{m=1}^{\infty} I_m\left(\frac{eU_0}{kT_e}\right) \cos(m\omega t) = \sum_{m=1}^{\infty} I_{m\omega} \left(\frac{eU_0}{kT_e}\right) \cos(m\omega t)$$

where $I_{m\omega} \left(\frac{eU_0}{kT_e}\right) = 2I_{si} I_m\left(\frac{eU_0}{kT_e}\right) / I_0\left(\frac{eU_0}{kT_e}\right)$ - amplitude of m^{th} harmonic

$I_k(z)$ - Bessel functions of integer order k

For $eU_0/kT_e \ll 1$: $I_1\left(\frac{eU_0}{kT_e}\right) \approx \frac{eU_0}{2kT_e}$ $I_2\left(\frac{eU_0}{kT_e}\right) \approx \frac{1}{8} \left(\frac{eU_0}{kT_e}\right)^2$

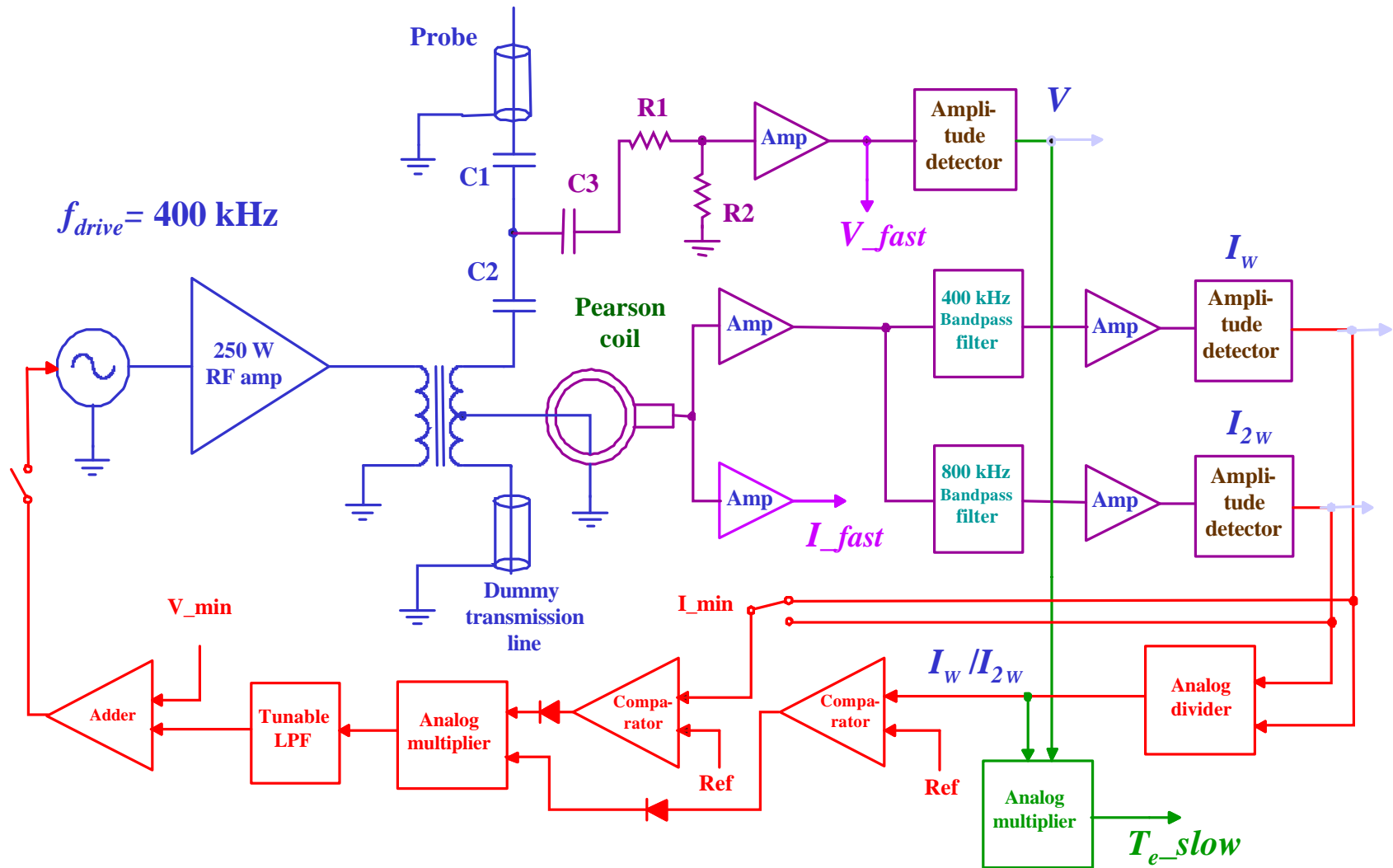
$$kT_e \approx \frac{eU_0}{4} \frac{I_1}{I_2} = \frac{eU_0}{4} \frac{I_{\omega}}{I_{2\omega}}$$

Thus T_e can be determined from the ratio of the amplitudes of 1st and 2nd harmonics

The error of this approximation for $eU_0/kT_e = 1$ is only about 5% [1]

[1] Boedo *et al*, Rev. Sci. Instrum. **70** (1999), 2997

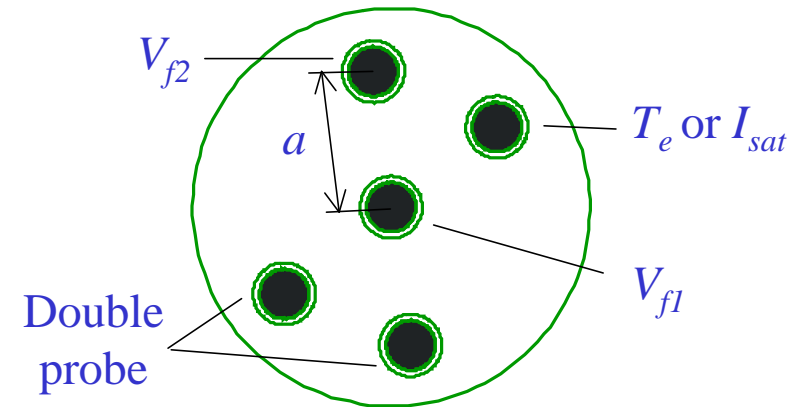
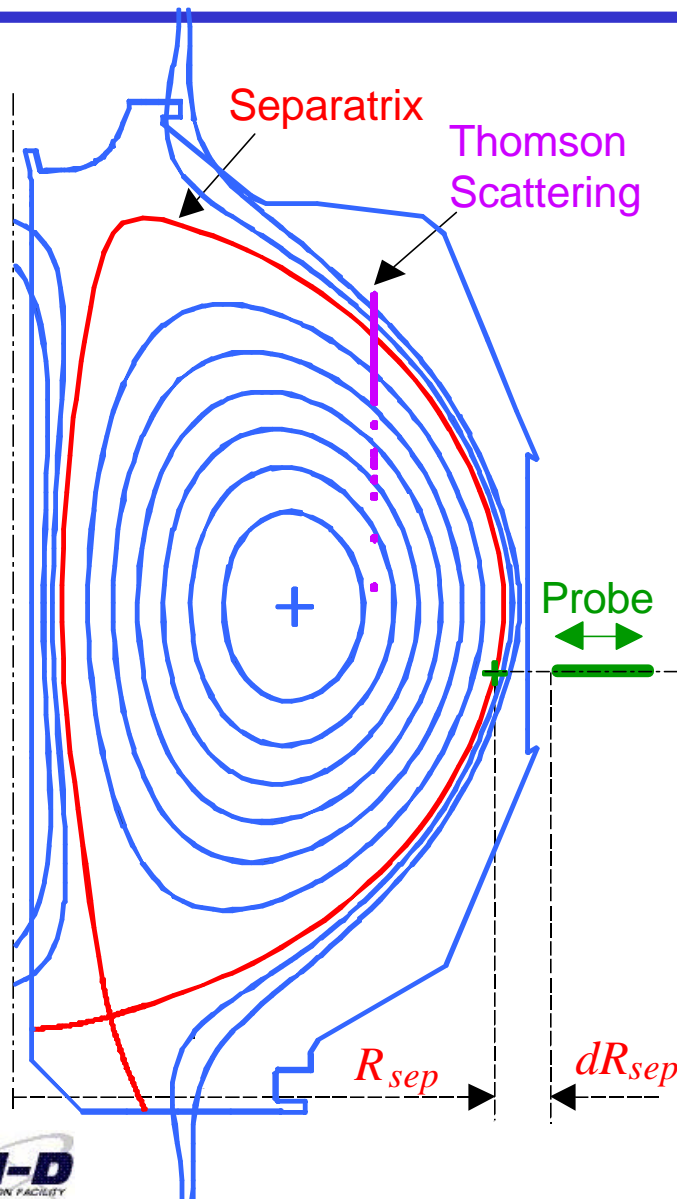
Harmonic Diagnostic on DIII-D



Novel Features of the Harmonic Diagnostic on DIII-D

- Fully digital data processing for improved phase resolution:
 - * Raw voltage and current signals are digitized at a sample rate of 5 MHz
 - * Amplitudes of current harmonics are extracted by digital filtering
 - * This digital procedure does not introduce phase delays
- Active drive voltage feedback for improved dynamic range:
 - * Ratio of the amplitudes of 1st and 2nd current harmonics is determined in real time using an analog divider
 - * This ratio is kept within preset limits $4 \leq I_{1W}/I_{2W} \leq 10$ by providing feedback to the function generator
- Real time T_e measurement for long pulse capability:
 - * An analog multiplier is used to multiply the ratio of the current harmonic amplitudes by the drive voltage amplitude producing a signal proportional to T_e
 - * This “slow” (about 10 kHz bandwidth) signal can be used to monitor T_e on long time scales

Experimental Arrangement on DIII-D



Probe head layout

Poloidal electric field is estimated as:

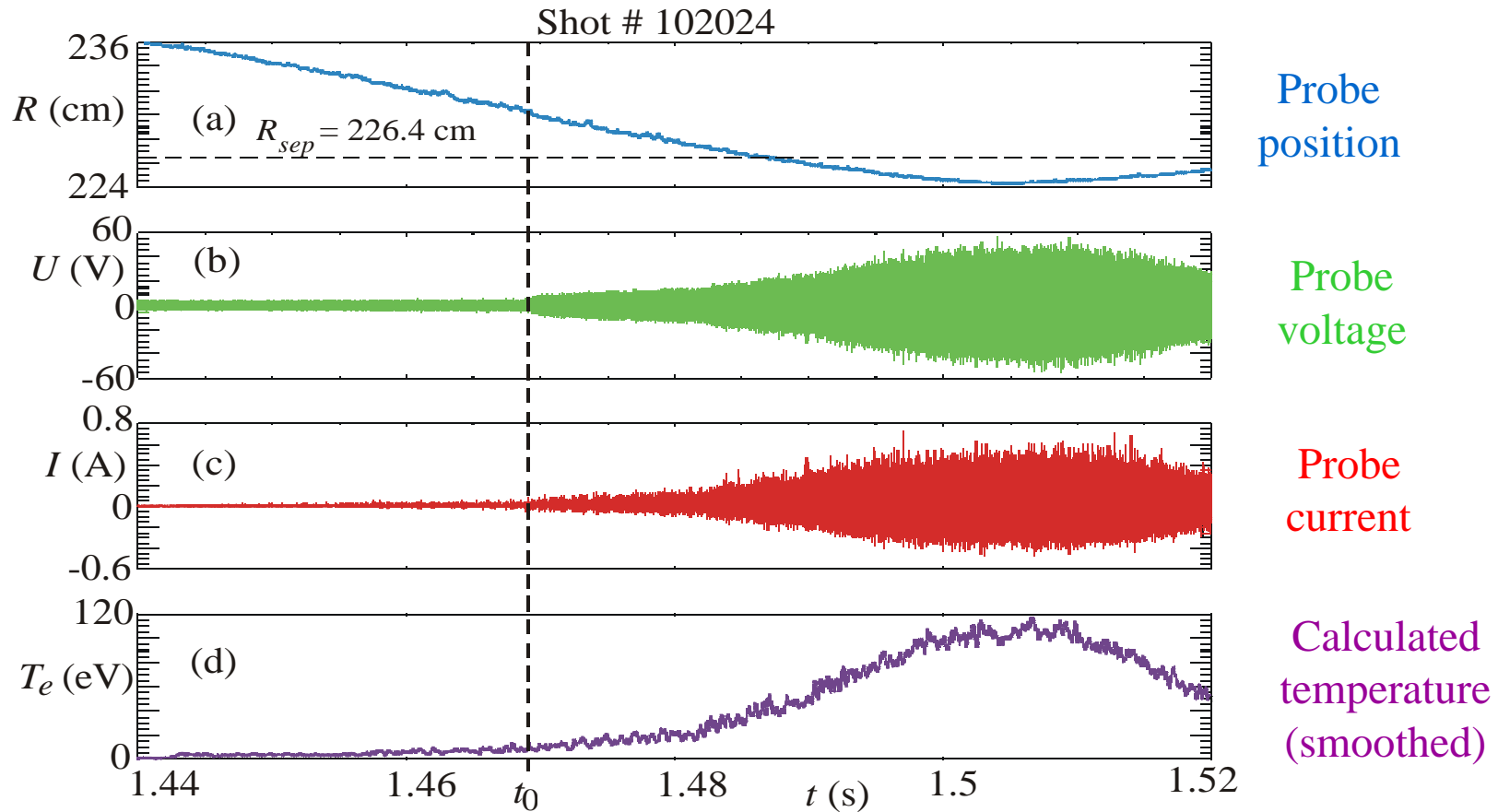
$$E_q \approx (V_{f2} - V_{f1}) / a$$

The total in-and-out (plunge) time is about 0.2 s

The total plunge length is about 15 cm

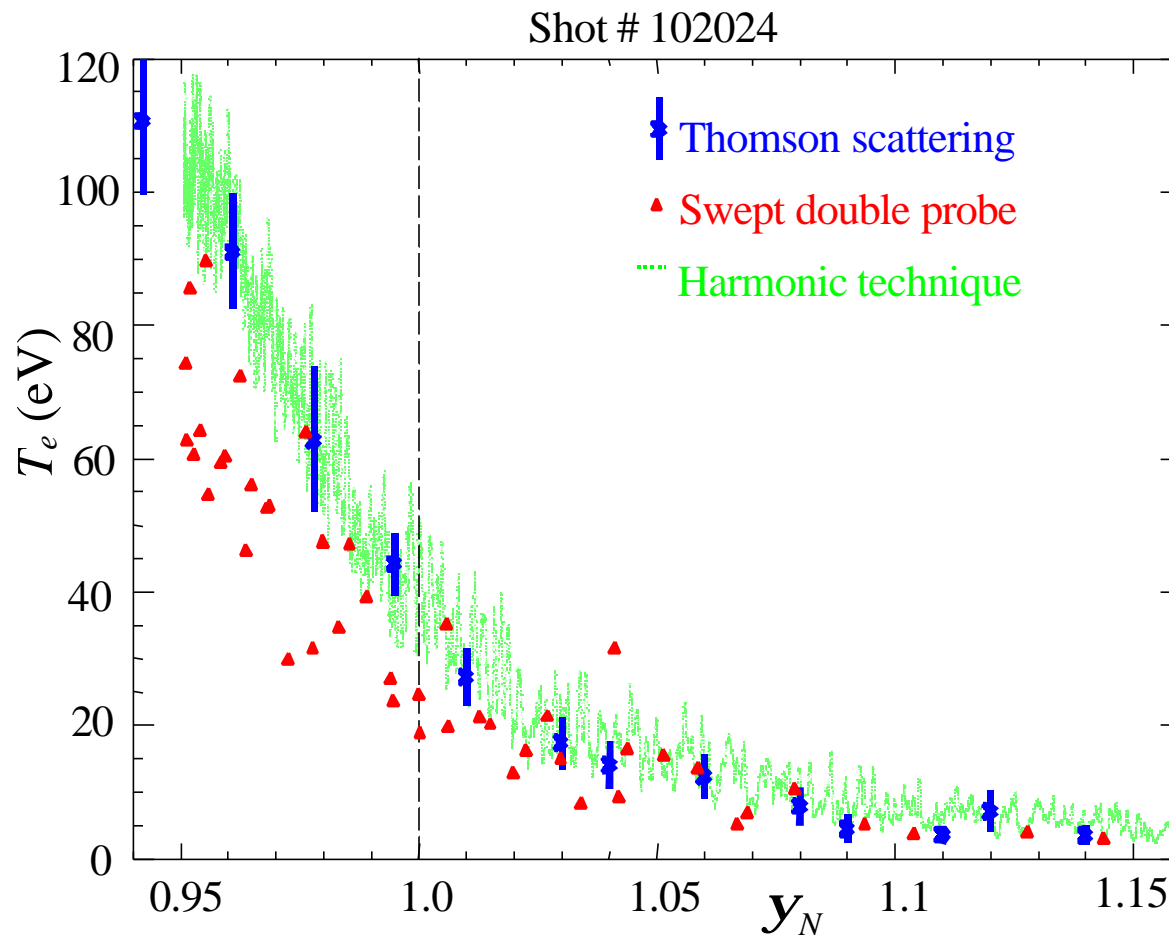
R_{sep} is the major radius of the separatrix (calculated by EFIT) at the probe location

Raw Signals and Calculated Temperature



At $t = t_0$ feedback turns on and keeps the ratio T_e/U within preset limits

Slow Time Scale: Comparison with Other Techniques

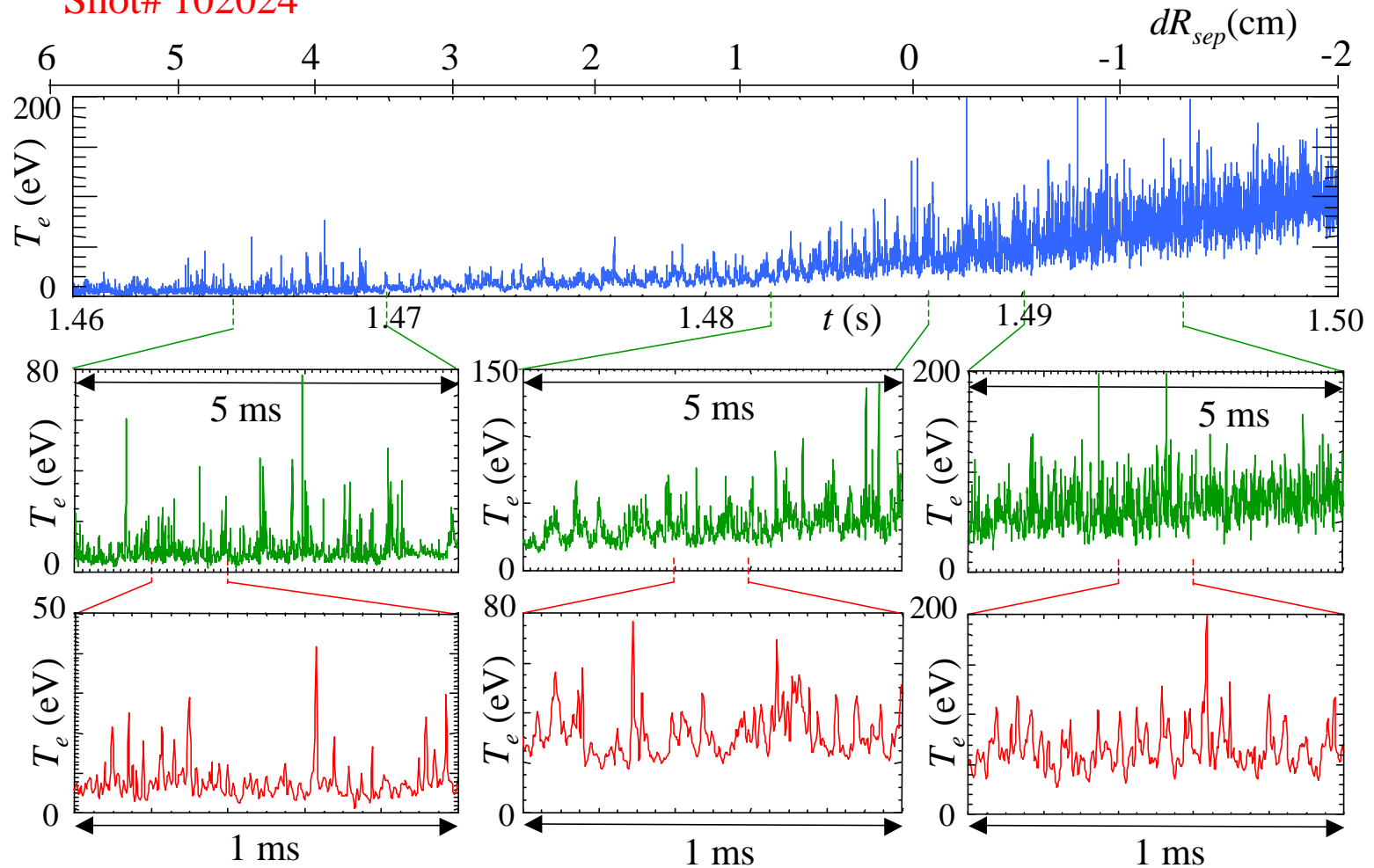


Harmonic technique and Thomson scattering are in good agreement throughout the range

Double probe is in agreement outside the separatrix, but gives lower temperatures inside the separatrix

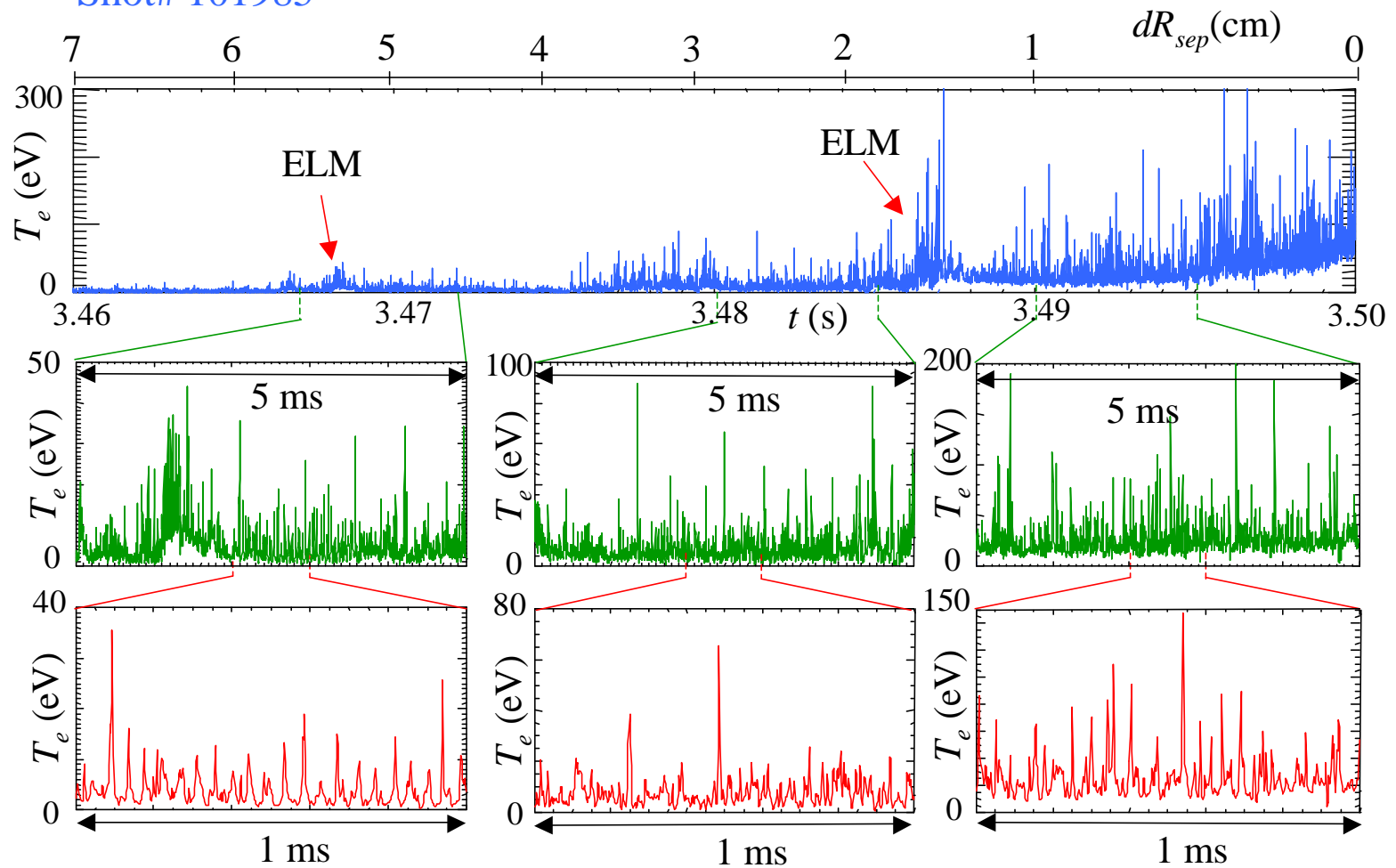
Edge Electron Temperature Fluctuations in L-mode

Shot# 102024



Edge Electron Temperature Fluctuations in H-mode

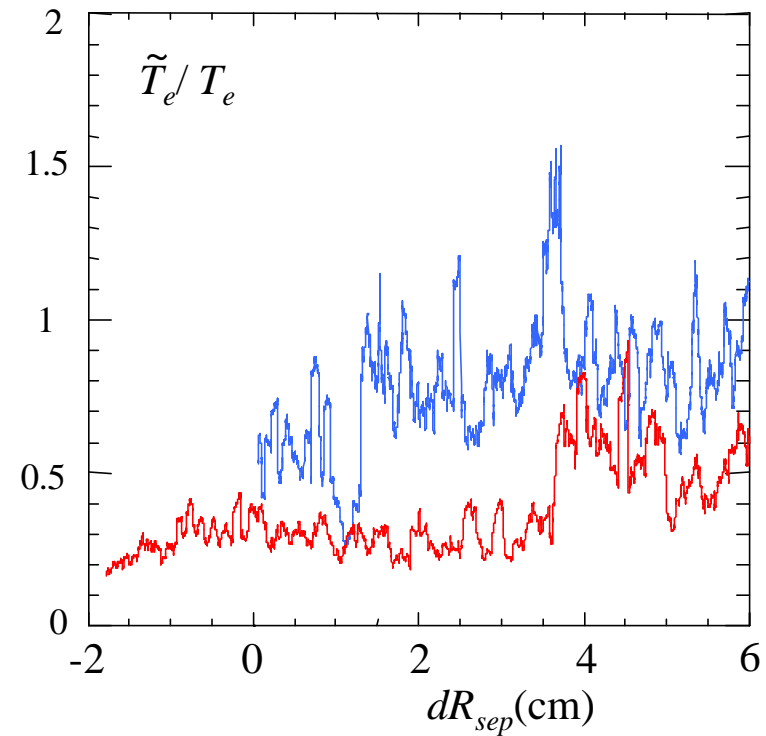
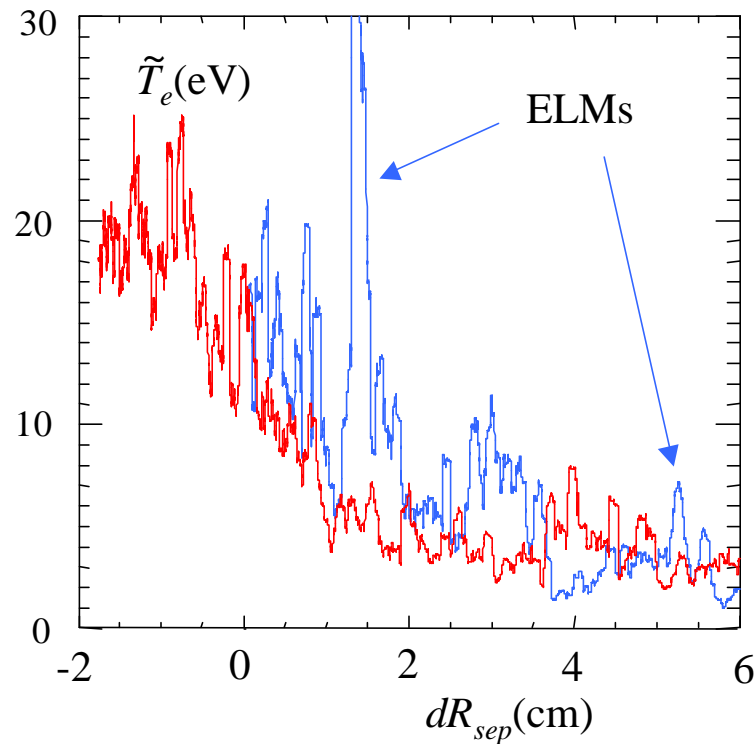
Shot# 101985



Absolute and Relative T_e Fluctuation Levels in L- and H-modes

— L-mode, Shot# 102024

— H-mode, Shot# 101985



Absolute T_e fluctuation levels are comparable in L- and H-modes

Relative T_e fluctuation levels are higher in H-mode due to lower T_e

Statistical Moments

$$\text{Mean} = \bar{X} = \frac{1}{N} \sum_{j=0}^{N-1} X_{j-N/2}$$

Mean value,
SMOOTH in IDL

$$\text{Variance} = \mathbf{s}^2 = \frac{1}{N} \sum_{j=0}^{N-1} (X_{j-N/2} - \bar{X})^2$$

Square of RMS
amplitude

$$\text{Skewness} = S = \frac{1}{N} \sum_{j=0}^{N-1} \left(\frac{X_{j-N/2} - \bar{X}}{\mathbf{s}} \right)^3$$

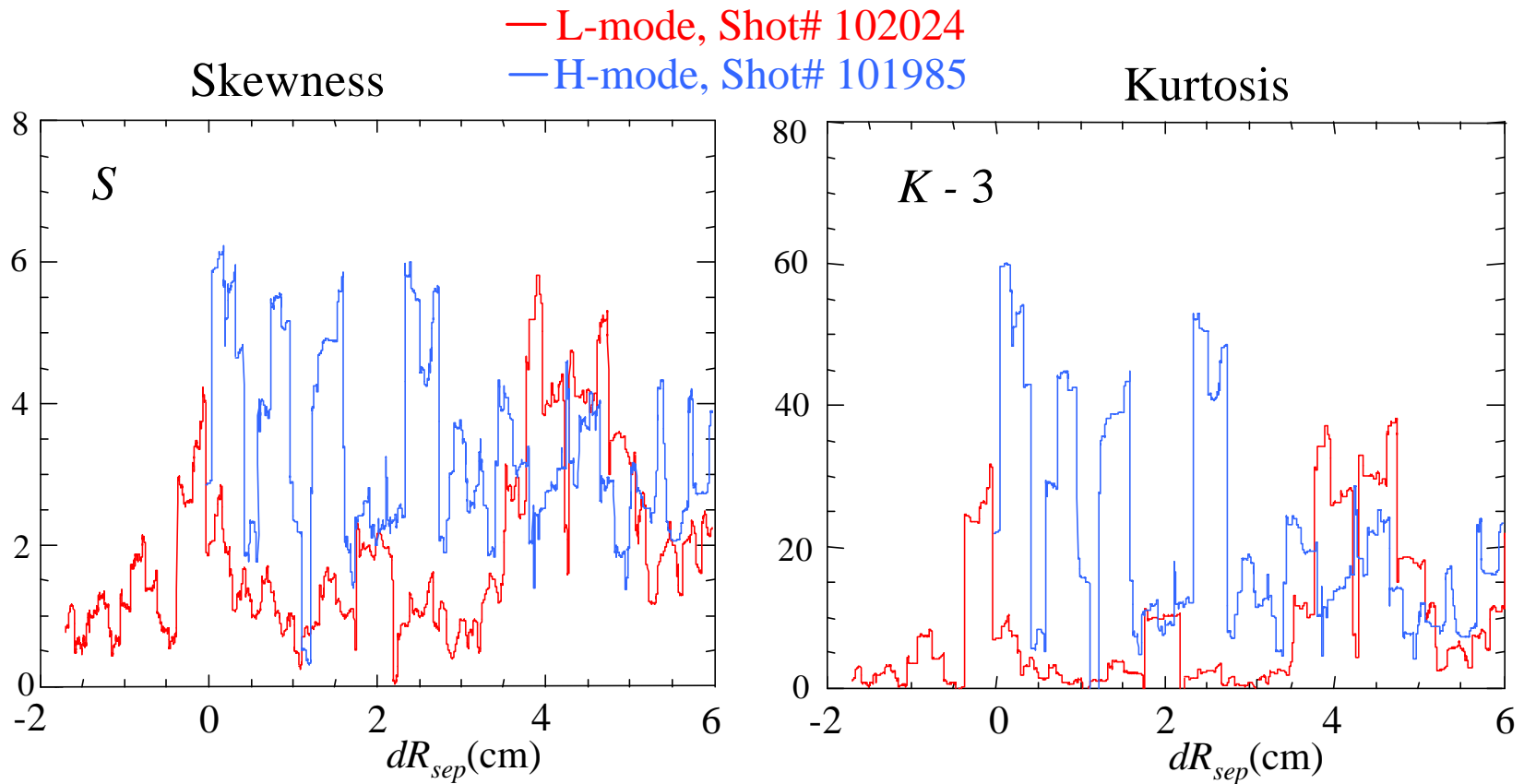
Measure of asymmetry
of the PDF;
for Gaussian PDF $S = 0$

$$\text{Kurtosis} = K = \frac{1}{N} \sum_{j=0}^{N-1} \left(\frac{X_{j-N/2} - \bar{X}}{\mathbf{s}} \right)^4$$

Measure of flatness of
the PDF;
for Gaussian PDF $K = 3$

All the above moments can be calculated in any point i
of an array using N adjacent points from $i-N/2$ to $i+N/2$

Skewness and Kurtosis of T_e Fluctuations in L- and H-modes



T_e fluctuations statistics is non-Gaussian in both L- and H-modes with the deviation being smaller in L-mode

Spikes in T_e , Real or Not?

The observed spikes in T_e may be:

- real
- due to secondary electron emission caused by fast ions, X-rays, UV, etc
- due to poor signal to noise ratio

Since $\mathbf{j}_f = \mathbf{j}_p - \mathbf{a} kT_e/e$ where $\mathbf{a} \sim 3$, T_e spikes shall translate in V_f

- If a T_e spike is **real**, V_f is likely to have a **negative spike**
- If a T_e spike is **due to the secondary emission**, V_f is likely to have a **positive spike**
- If a T_e spike due to **poor signal to noise ratio**, V_f is likely to have **no spike**

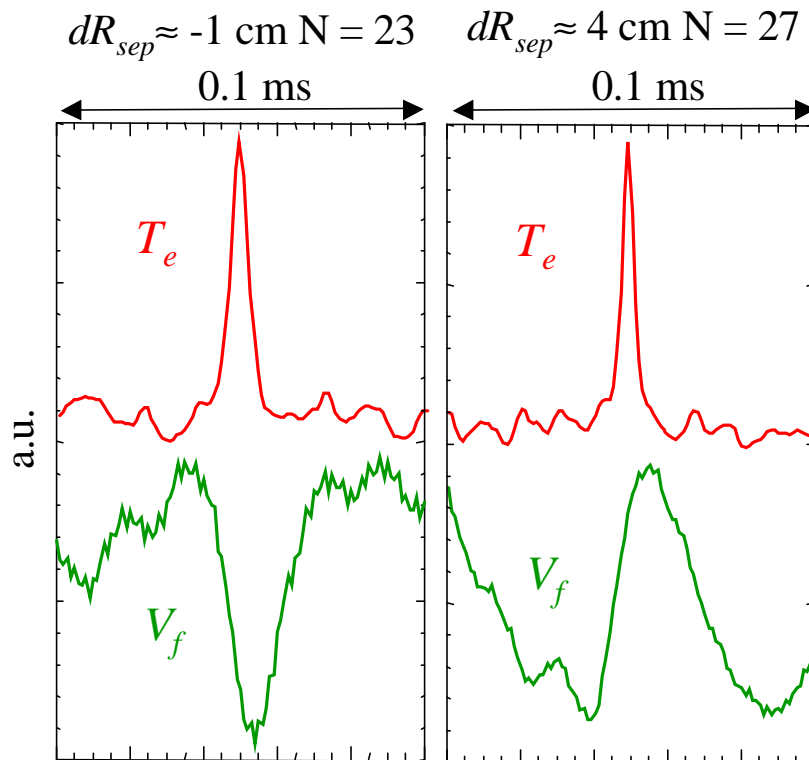
This can be checked using **conditional averaging**:

- Spikes in T_e above certain level are found for a given time interval
- T_e and V_f data are averaged around the spikes

Conditional Averaging of T_e and V_f

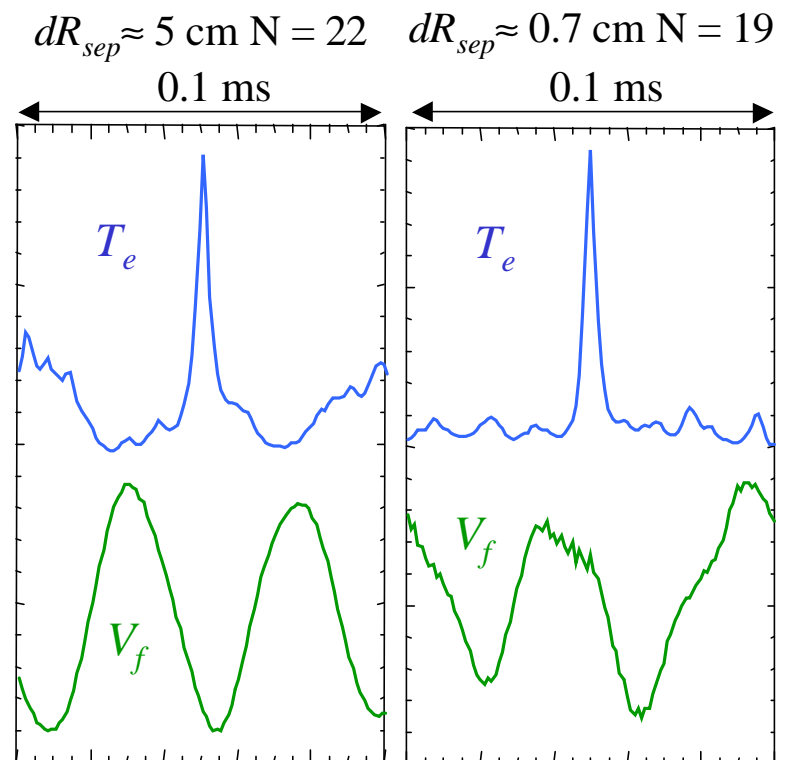
L-mode, Shot# 102024

H-mode, Shot# 101985



Mostly real

Mostly emission



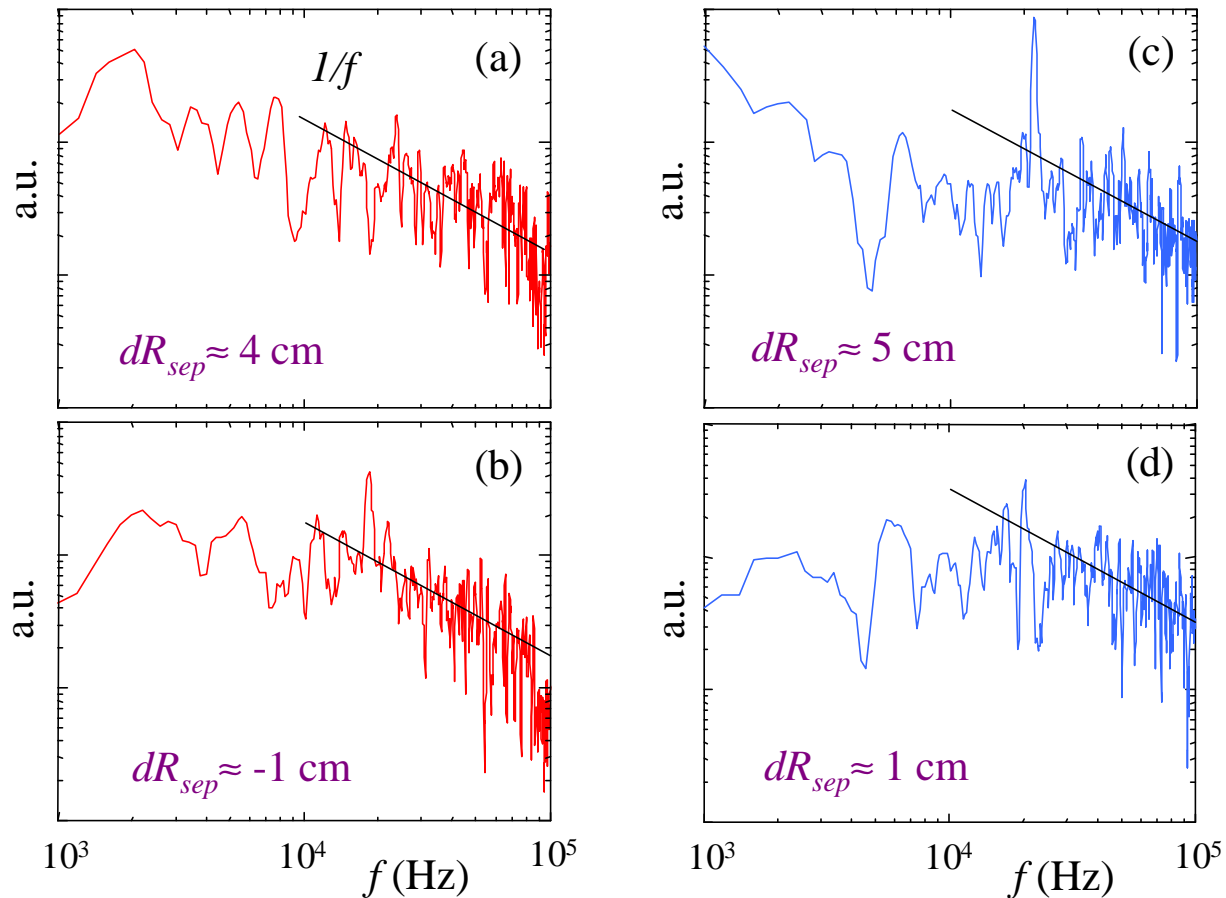
Real!
Coherent mode

Inconclusive

T_e Fluctuation Power Spectra in L- and H-modes

L-mode, Shot# 102024

H-mode, Shot# 101985

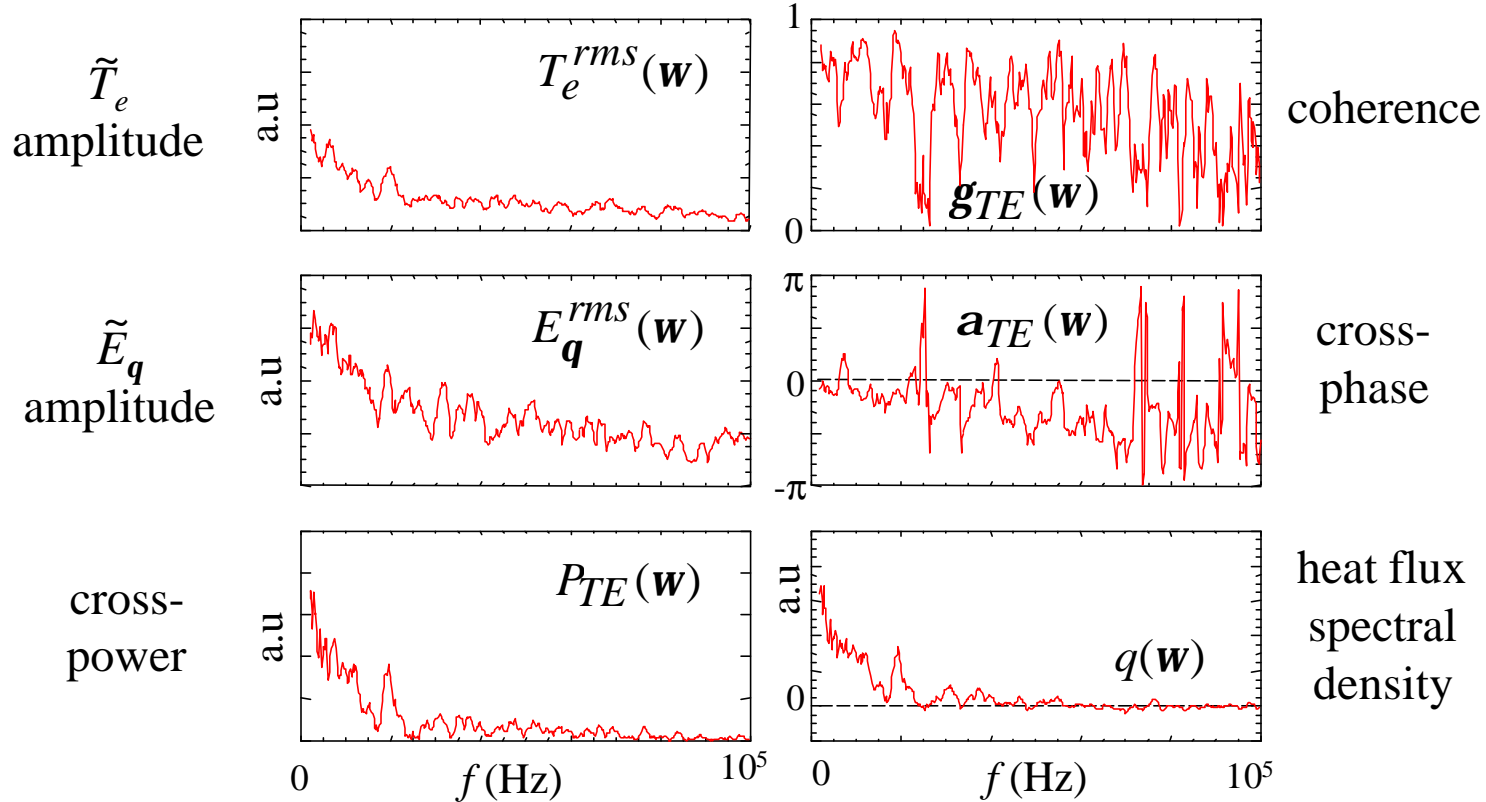


The $1/f$ dependence is best fitted to the spectrum inside the separatrix in L-mode (b)

Terms Contributing to Turbulent Heat Flux, L-mode

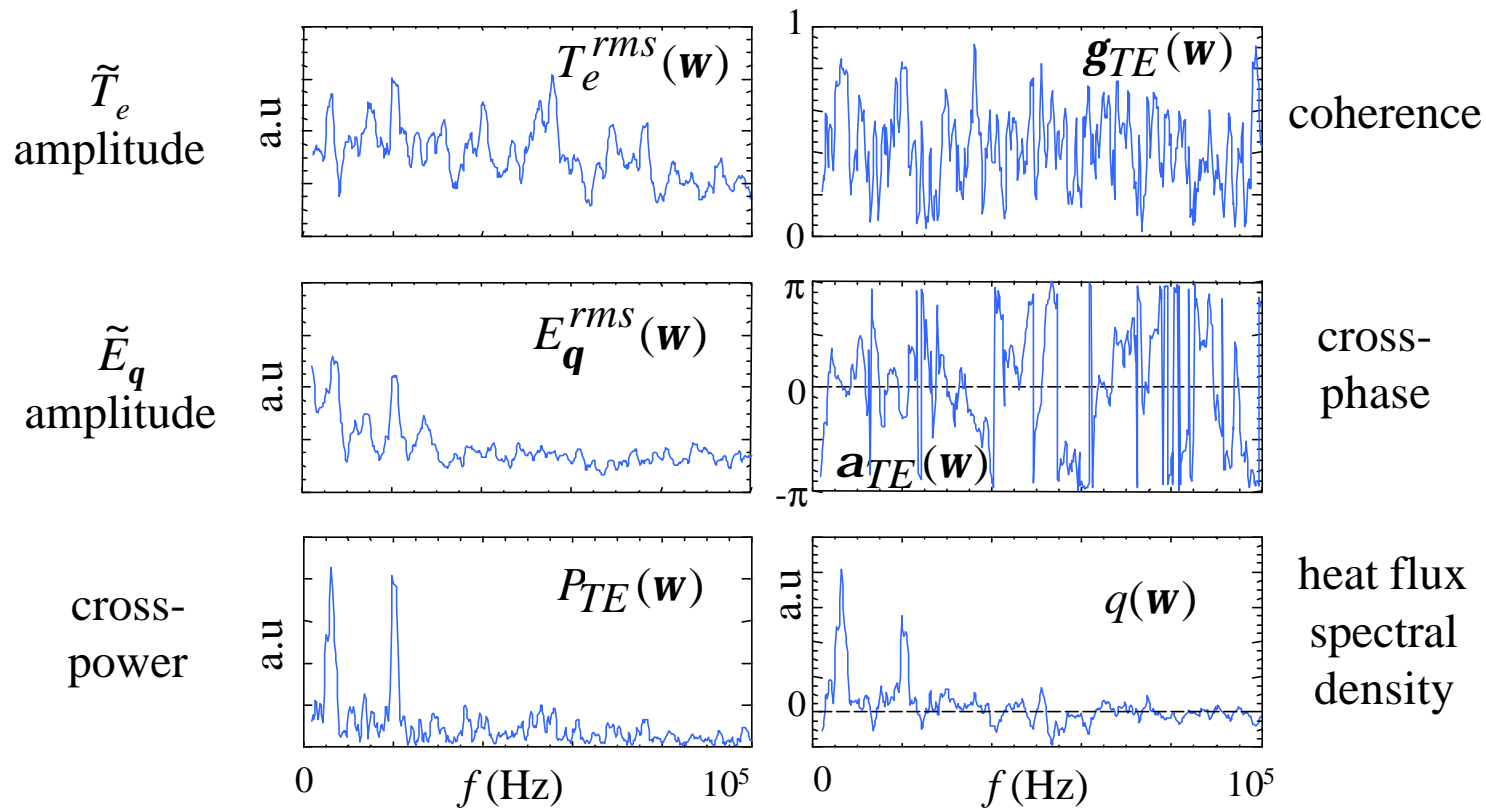
$$Q_{cond} = \int_0^{\infty} q(\omega) d\omega, \quad q(\omega) = \frac{3}{2} \frac{n_e}{B_j} \underbrace{T_e^{rms}(\omega) E_q^{rms}(\omega) g_{TE}(\omega)}_{P_{TE}(\omega)} \cos(a_{TE}(\omega))$$

Shot# 102024, dRsep \approx 0.5 - 0 cm



Terms Contributing to Turbulent Heat Flux, H-mode

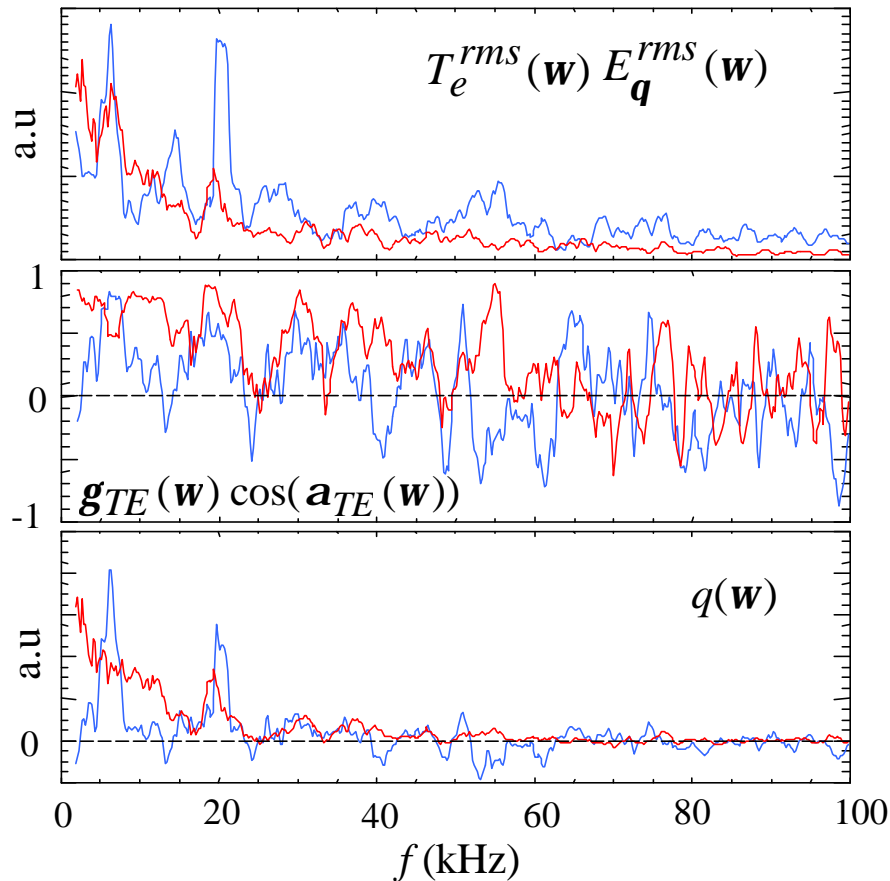
Shot# 101985, dRsep \approx 0.5 - 0 cm



Amplitude of the temperature fluctuations is higher in H-mode throughout the frequency spectrum!

Turbulent Heat Flux is Lower in H-mode Due to Worse Correlation of Fluctuations

— L-mode, Shot# 102024
— H-mode, Shot# 101985



Product of the fluctuation amplitudes is higher in H-mode throughout most of the spectrum

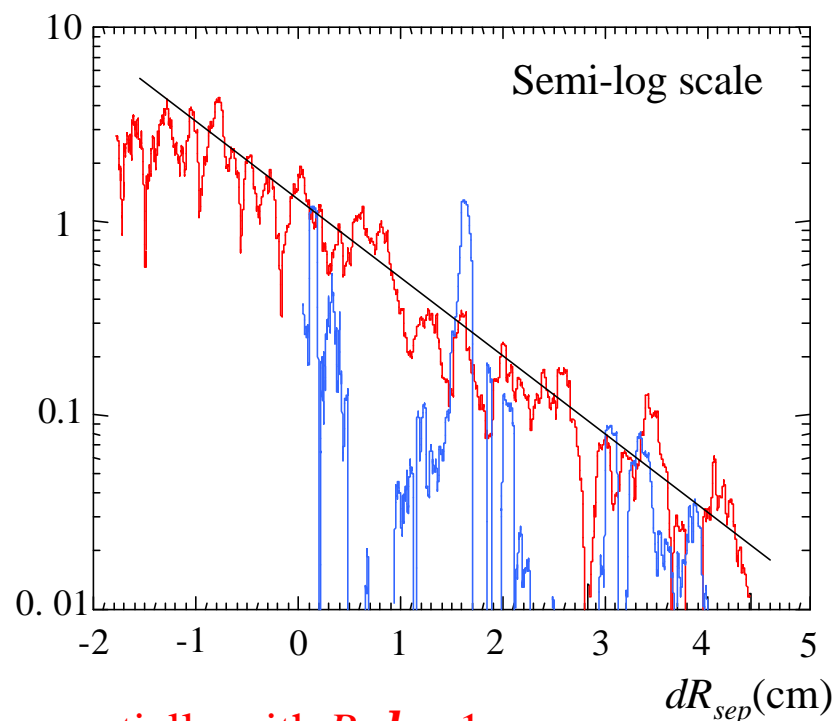
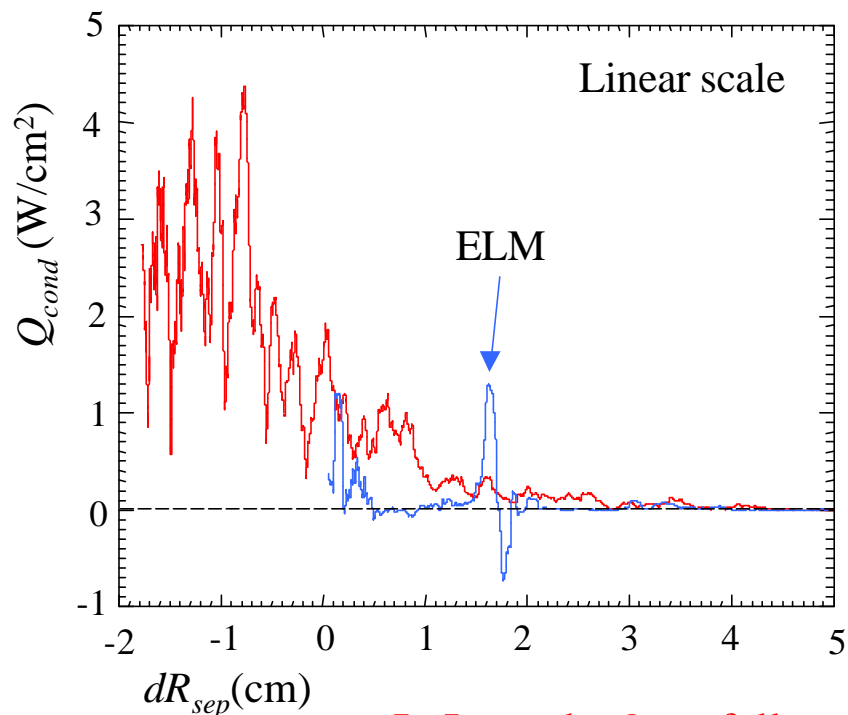
Fluctuations are better correlated in L-mode at low frequencies ($f < 40$ kHz) except for a couple of quasi-coherent peaks in H-mode

Total conducted heat flux is about 3 times higher in L-mode!

Radial Profiles of Conductive Heat Flux in L- and H- modes

Conductive heat flux can be calculated in time domain: $Q_{cond}^{ES} = \frac{3}{2} \frac{n_e}{B_j} \langle k \tilde{T}_e \tilde{E}_q \rangle$

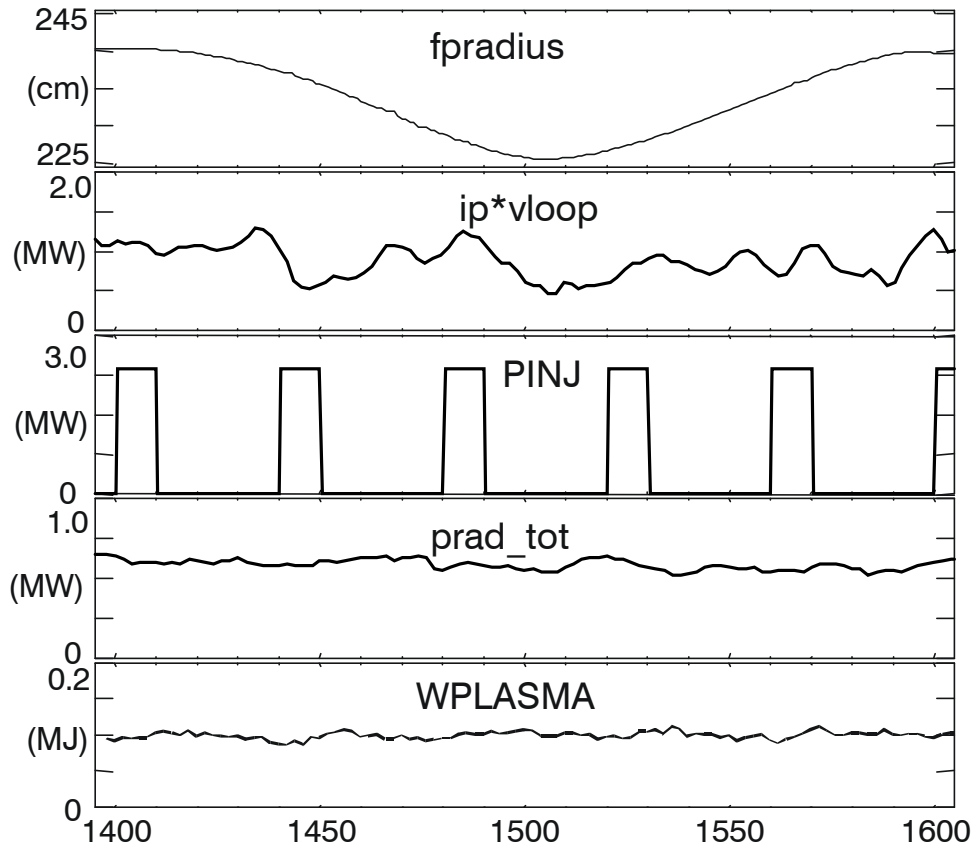
— L-mode, Shot# 102024
— H-mode, Shot# 101985



In L-mode Q_{cond} falls exponentially with R , $l \approx 1$ cm

Conductive Heat Flux and Power Balance, L-mode

Shot# 102024



Average NBI power:

$$\langle P_{NBI} \rangle \approx 0.6 \text{ MW}$$

Total input power:

$$P_{in} = P_{NBI} + P_{Ohmic} \approx 1.6 \text{ MW}$$

Radiated power:

$$P_{rad} \approx 0.6 \text{ MW}$$

Power conducted through
the last closed flux surface
(taking $Q_{cond} \approx 1.5 \text{ W/cm}^2$)

$$P_{cond} = Q_{cond} S_{LCFS} \approx 0.8 \text{ MW}$$

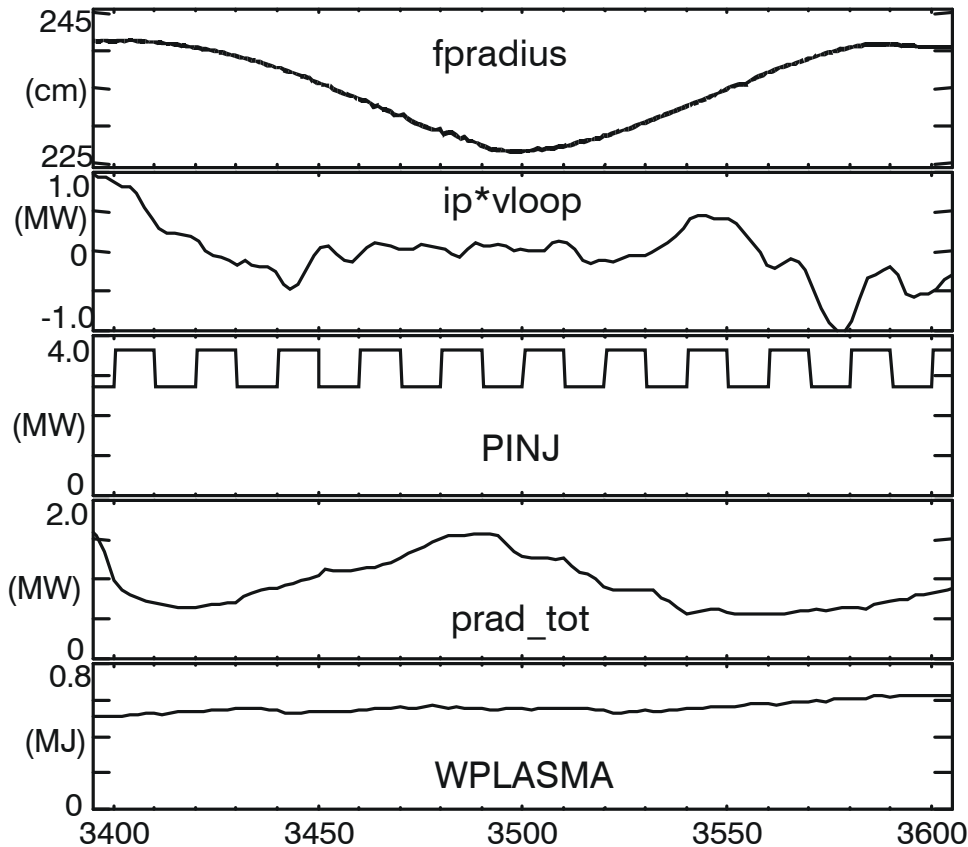
Same order of magnitude:

$$P_{cond} \sim P_{in} - P_{rad}$$

Contribution of Q_{cond} to power balance is important in L-mode

Conductive Heat Flux and Power Balance, H-mode

Shot# 101985



Average NBI power:

$$\langle P_{NBI} \rangle \approx 3.6 \text{ MW}$$

Total input power:

$$P_{in} = P_{NBI} + P_{Ohmic} \approx 3.6 \text{ MW}$$

Radiated power:

$$P_{rad} \approx 1.5 \text{ MW}$$

Power conducted through
the last closed flux surface
(taking $Q_{cond} \approx 0.3 \text{ W/cm}^2$)

$$P_{cond} = Q_{cond} S_{LCFS} \approx 0.16 \text{ MW}$$

**Conducted power is
relatively small :**

$$P_{cond} \ll P_{in} - P_{rad}$$

Contribution of Q_{cond} to power balance is small in H-mode

Summary

- Electron temperature fluctuations with relative levels of 0.3 - 0.5 near the separatrix and 0.5 - 0.8 in the scrape-off layer are present in both L- and H-modes
- Absolute T_e fluctuation levels are close in L- and H-modes, while relative levels are higher in H-mode
- T_e fluctuation spectra may have regions consistent with $1/f$ dependence with best fit obtained inside the separatrix in L-mode
- T_e fluctuation statistics is non-Gaussian in both L- and H-modes. The deviation from Gaussian statistics is larger in H-mode
- T_e and E_q fluctuations are better correlated in L-mode at low frequencies ($f < 40$ kHz).
- Quasi-coherent peaks are observed in T_e and E_q spectra in H-mode
- Conductive turbulent heat flux is considerably higher in L-mode
- Contribution of the conductive turbulent heat flux to the power balance is significant in L-mode and small in H-mode